

## MATERIALS SCIENCE

# Rationalizing phonon dispersion for lattice thermal conductivity of solids

Zhiwei Chen<sup>1</sup>, Xinyue Zhang<sup>1</sup>, Siqi Lin<sup>1</sup>, Lidong Chen<sup>2,\*</sup> and Yanzhong Pei<sup>1,\*</sup>

## ABSTRACT

Lattice thermal conductivity ( $\kappa_L$ ) is one of the most fundamental properties of solids. The acoustic–elastic-wave assumption, proposed by Debye (Debye P. *Ann Phys* 1912; 344: 789–839), has led to linear phonon dispersion being the most common approximation for understanding phonon transport over the past century. Such an assumption does not take into account the effect of a periodic boundary condition on the phonon dispersion, originating from the nature of periodicity on atomic arrangements. Driven by modern demands on the thermal functionality of materials, with  $\kappa_L$  ranging from ultra-low to ultra-high, any deviation from the Debye approximation in real materials becomes more and more significant. This work takes into account the periodic boundary condition, and therefore rationalizes the phonon dispersion to be more realistic. This significantly improves the precision for quickly predicting  $\kappa_L$  without any fitting parameters, as demonstrated in hundreds of materials, and offers a theoretical basis rationalizing  $\kappa_L$  to be lower than the minimum currently accepted based on the Debye dispersion. This work paves the way for designing solids with expected  $\kappa_L$  and particularly inspires the advancement of low- $\kappa_L$  materials for thermal energy applications.

**Keywords:** thermoelectric, thermal conductivity, minimal thermal conductivity, phonon dispersion

## INTRODUCTION

Lattice thermal conductivity ( $\kappa_L$ ) strongly affects the applications of materials related to thermal functionality, such as thermal management [1], thermal barrier coatings [2] and thermoelectrics [3–5].  $\kappa_L$  is determined by the specific heat ( $c_V$ ), phonon group velocity ( $v_g$ ) and phonon relaxation time ( $\tau$ ), which are all strongly linked to the dispersion of phonons. By manipulating these physical parameters, many different materials either with ultra-low or ultra-high  $\kappa_L$  have been successfully made [6–8].

In cases of applications that require a low  $\kappa_L$ , such as thermoelectrics, complex crystal structures are usually focused on. This is because an increase of the number of atoms in a primitive cell folds the high-frequency portion of phonons back into the first Brillouin zone as optical ones with significantly reduced group velocities. This reduces the fraction of acoustic phonons, which is equivalent to the effect of reducing the acoustic specific heat for  $\kappa_L$ -reduction, since acoustic phonons are the dominant contributors to  $\kappa_L$  because of their high group velocities [8–12].

Alternatively, both introducing defects with different dimensionalities (0D point defects [13–17], 1D dislocations [18–21] and 2D interfaces [22,23]) and utilizing the strong lattice anharmonicity [24–27] help to shorten the overall phonon relaxation time ( $\tau$ ). In addition, a weak bonding force in materials with heavy elements leads to a small slope of phonon frequency versus wave vector, meaning a small group velocity ( $v_g$ ) for phonons [28,29].

In cases of applications that require a high  $\kappa_L$ , carbon materials such as 3D diamond [30], 2D graphene [31] and 1D carbyne in the form of cumulene [32] have strong C–C chemical bonds, light atomic mass and small primitive cells and therefore show the highest  $\kappa_L$  among known solids.

In order to understand the lattice thermal conductivity more quantitatively and in a time- and cost-effective way, many researchers devoted their efforts to it and developed a few physical models using approximated phonon dispersions over the past century [33–45] (see the supplementary section entitled ‘Development of modeling lattice thermal

<sup>1</sup>Interdisciplinary Materials Research Center, School of Materials Science and Engineering, Tongji University, Shanghai 201804, China and <sup>2</sup>State Key Lab of High Performance Ceramics & Superfine Microstructures, Shanghai Institute of Ceramics, Chinese Academy of Sciences, Shanghai 200050, China

\*Corresponding authors. E-mails: [cld@mail.sic.ac.cn](mailto:cld@mail.sic.ac.cn); [yanzhong@tongji.edu.cn](mailto:yanzhong@tongji.edu.cn)

Received 29 June 2018; Revised 23 August 2018;

Accepted 3 September 2018

conductivity'). Most [33–40,45] of these models use a linear phonon dispersion, as proposed by Debye in 1912 based on an acoustic–elastic-wave assumption [46], while other models either involve mathematical fitting parameters on phonon dispersion [41–43] or lack detailed equations for phonon transport properties [44]. The linear phonon dispersion of Debye offers many simplifications on phonon transport properties, and was the most common approximation in the past. The Debye dispersion successfully predicts a  $T^3$  dependence of the heat capacity ( $C_V$ ) at low temperatures and  $C_V$  approaches the Dulong–Petit limit at high temperatures.

However, the nature of periodicity on atomic arrangements leads to a periodic boundary condition for lattice vibrations in solids, which actually creates lattice standing waves at Brillouin boundaries. This does not satisfy the acoustic–elastic-wave assumption of Debye, as proposed by Born and von Karman (BvK) in 1912 [47]—the same year that Debye proposed the linear dispersion [46]. This results in a significant deviation of Debye dispersion for periodic crystalline materials when phonons with wave vectors are close to the Brillouin boundaries (high-frequency phonons; see the supplementary section entitled 'Detailed deduction on phonon transport properties'). When these phonons are involved for phonon transport (i.e. at not extremely low temperatures), Debye dispersion leads to an overestimation of lattice thermal conductivity because of the overestimation of the group velocity for these high-frequency phonons, as observed in materials with known measured  $\kappa_L$  and necessary details for a time- and cost-effective model prediction to our best knowledge (Fig. 1g and h show a mean absolute deviation of +40% and 35%). In addition, Debye dispersion overestimates the theoretically available lower bound of lattice thermal conductivity ( $\kappa_{L,\min}$ ) as well, leading the violations of the measured  $\kappa_L$  to be even lower than the  $\kappa_{L,\min}$  predicted (Debye–Cahill model) [48] to be observed in tens of materials (Fig. 2).

This work takes into account the BvK boundary condition [47], and reveals that the product of acoustic and optical dispersions yields a sine function (see the supplementary section entitled 'Detailed deduction on phonon transport properties'). In the case in which the mass (or the force constant) contrast between atoms is large, the acoustic dispersion tends to be a sine-function (Fig. S1). This sine-type dispersion indeed exists in both the simplest [32] and the most complex materials [49] (see the supplementary section entitled 'Detailed deduction on phonon transport properties'). Approximating the acoustic dispersion to be sine, the BvK boundary condition subsequently reduces the remaining

optical branches to a series of localized modes with a series of constant frequencies. It should be noted that, with the development of computation technology, first-principles calculations could enable a more detailed phonon dispersion. However, this is usually time-consuming and computationally expensive, particularly for materials with imperfections. It is therefore still significant nowadays if a rationalized phonon dispersion is developed for a time- and cost-effective prediction of phonon transport.

This work utilizes the above-mentioned rationalization of phonon dispersion, which enables both contributions to  $\kappa_L$  of acoustic and optical phonons to be included. This improvement in phonon dispersions significantly improves the accuracy of a time- and cost-effective prediction on  $\kappa_L$  of solids (Fig. 1c, showing a mean absolute deviation of only -2.5%), and therefore offers a more precise design of solids with expected  $\kappa_L$ . Furthermore, this work successfully removes the contradiction of the measured  $\kappa_L$  being even lower than the minimum ( $\kappa_{L,\min}$ , predicted based on a Debye dispersion, Fig. 2). This would provide the theoretical possibility of rationalizing  $\kappa_L$  to be lower than is currently thought, opening further opportunities for advancing thermally resistive materials for applications, such as thermoelectrics.

## RESULTS AND DISCUSSION

The similarity between the linear dispersion proposed by Debye and the one developed in this work lies in the region of acoustic phonons having low frequencies (wave vectors close to the Brillouin zone center, the  $\Gamma$  point). This leads both dispersions to predict a  $T^3$  dependence of heat capacity ( $C_V$ ) at low temperatures (Fig. S3). The overall phonon frequency from a linear dispersion is higher than that from the dispersion developed in this work, which reduces the probability of phonons being excited and therefore leads to a lower  $C_V$ , particularly at mid-temperatures (Fig. S3). In the high-temperature limit, available phonons of any dispersions are completely excited, leading the energy carried by each atom to be  $3k_B T$  (known as the Dulong–Petit law, Fig. S3) in bulk solids [50] excluding those with liquid-like species [51,52].

The most successful models without any fitting parameters for a time- and cost-effective prediction of the intrinsic  $\kappa_L$  (with Umklapp scattering only) of crystalline solids are those developed by Slack in 1973 [53], with improvements by Klemens [54], and by Snyder in 2011 [45]. Both models are based on a linear phonon dispersion of Debye for acoustic phonons, and are therefore called

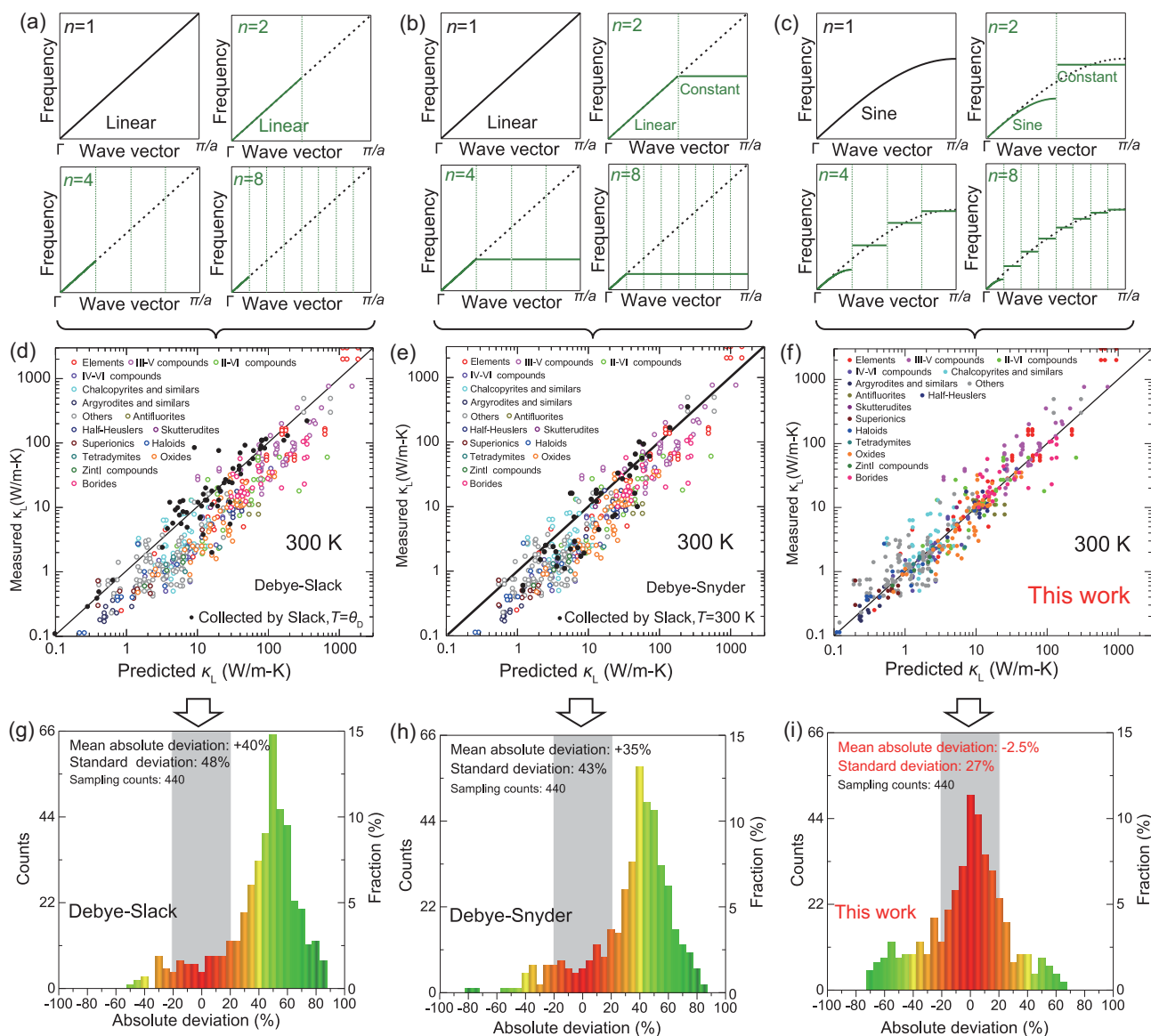


**Figure 1.** Comparison of phonon dispersion (a, b and c), measured lattice thermal conductivity versus prediction (d, e and f) and the corresponding error analyses (g, h and i) for the Debye–Slack model (a, d and g), the Debye–Snyder model (b, e and h) and the one developed in this work considering the periodic boundary condition (c, f and i) for crystalline solids. Details of the materials involved are given in Table S1.

in this work the Debye–Slack and Debye–Snyder models, respectively. The difference between them is that Slack only considers the contribution of acoustic phonons (Fig. 1a) while Snyder assumes that all optical phonons have the cut-off frequency of the acoustic branch (Fig. 1b). The phonon dispersion developed in this work, taking into account the periodic boundary condition, is shown in Fig. 1c.

In order to better evaluate the accuracy of each time- and cost-effective model prediction to the best of our ability, a total of  $\sim 450$  measured room-temperature lattice thermal conductivities from  $\sim 300$  different materials are collected for comparison (similar results for other temperatures

can be expected since they strictly follow a  $T^{-1}$  dependence due to Umklapp scattering; see the supplementary section entitled ‘Comparison on  $\kappa_L$  predicted by a Debye–Snyder model and the one developed in this work’). In the case of a linear dispersion, both the Debye–Slack (Fig. 1d) and Debye–Snyder (Fig. 1e) models statistically overestimate  $\kappa_L$  (by  $\sim 37\%$ , Fig. 1). This work successfully enables a removal of such a  $\kappa_L$ -overestimation (Fig. 1f). This can largely be understood by the overestimated acoustic phonon group velocity (particularly at high frequencies; see the supplementary sections entitled ‘Comparison on  $\kappa_L$  predicted by a Debye–Snyder model and the one developed in this work’ and ‘Discussion on  $\kappa_{L,\min}$ -

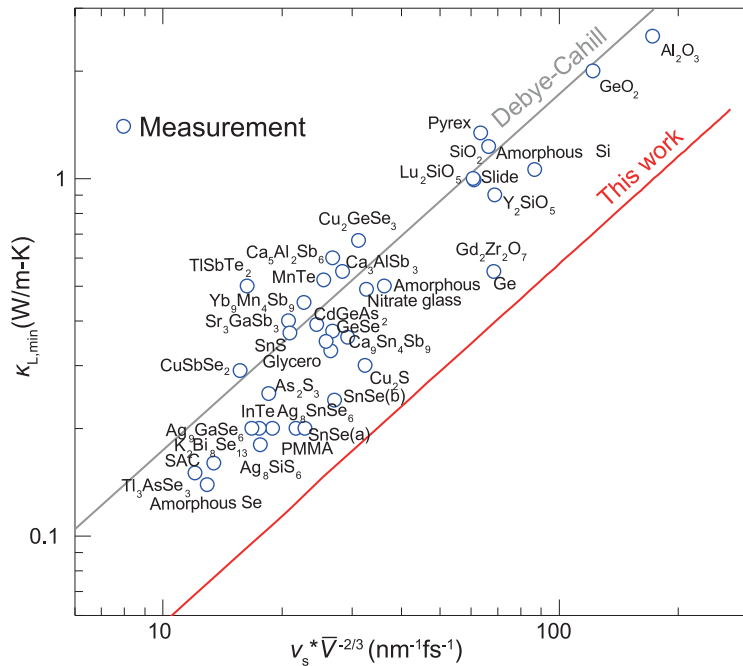


**Figure 2.** Comparison of measured minimal lattice thermal conductivity ( $\kappa_{L,\min}$ ) and predictions based on a dispersion developed according to the periodic boundary condition or on a linear dispersion of Debye (Debye–Cahill model). Details of the materials involved are given in Table S1.

prediction’) in the Debye–Slack and Debye–Snyder models, since acoustic phonons are the main contributors to  $\kappa_L$  [8,55].

In statistics (see the supplementary section entitled ‘Comparison on  $\kappa_L$  predicted by a Debye–Snyder model and the one developed in this work’), based on a linear dispersion of Debye and further including the contribution of optical phonons (Fig. 1b), Snyder’s model reduces both the mean absolute deviation (MAD) and the standard deviation (SD) by 5% statistically, as compared to Slack’s (Fig. 1g and 1h). This improvement indicates a weak contribution from optical phonons in general. This work successfully reduces MAD to be about zero (-2.5%, Fig. 1i), indicating that the phonon dispersion developed here indeed takes the major responsibility for  $\kappa_L$ -prediction. Such a significant improvement mostly comes from the development of the dispersion of acoustic phonons (sine versus linear), since all the models use the same scattering parameter (Grüneisen parameter, Table S1) and predict nearly the same heat capacity at high temperatures (Fig. S3).

The remaining SD of  $\sim 27\%$  (reduced from  $\sim 48\%$ ) in this work can be understood largely by the uncertainty of the Grüneisen parameter ( $\gamma$ ), measuring the strength of inherent Umklapp scattering. Its estimation can show a variation of 100% or higher from different sources even for a given material (Table S1), meaning a possible error as high as a factor of

4 or more for  $\kappa_L$ -prediction. This opens to the field the importance of the accuracy of  $\gamma$ -determination [24]. This work includes all available  $\gamma$  to the best of our knowledge from the literature on  $\kappa_L$ -prediction (Figs 1 and S4). However, if  $\gamma$  is unavailable, it is assumed to be 1.5, which is a statically averaged  $\gamma$  for known materials (Fig. S4). Note that usage of only the measured Grüneisen parameters from the available literature indeed enables a better prediction (Fig. S4 in the supplementary section entitled ‘Detailed deduction on phonon transport properties’).

In addition to inherent Umklapp scattering in solids, electron–phonon scattering resulting from a high carrier concentration (particularly in metal/semi-metals and extremely heavily doped semiconductors) as well as resonant scattering (in e.g. filled skutterudites and clathrates) can lead to a significant reduction in  $\kappa_L$ . Once the phonon relaxation time of this type of scattering is known,  $\kappa_L$  of these materials could be reasonably predicted as well, according to the model developed in this work.

As an extreme case of super-large  $n$ , typically meaning a super-big primitive cell,  $\kappa_L$  is expected to be extremely low [8,9], which is similar to the case of amorphous solids [48,56]. It should be noted that amorphous solids may show a reduced sound velocity and an enhanced phonon scattering for a lower  $\kappa_L$  as compared to those of crystalline ones, which can be understood by the existence of a distribution in interaction force resulting from the random atomic distance (see the supplementary section entitled ‘Sound velocity of amorphous solids’).

Based on the phonon theory, when the scattering probability of phonons reaches its maximum, the relaxation time is minimized as half of the period of each phonon [57], leading to a minimal lattice thermal conductivity ( $\kappa_{L,\min}$ ). In 1989 Cahill [48] developed a model for predicting  $\kappa_{L,\min}$  based on a linear dispersion of Debye (the Debye–Cahill model), which is the most common model for a time- and cost-effective  $\kappa_{L,\min}$ -prediction. Due to a similar reason of an overestimation of the phonon group velocity (particularly at high frequencies in a linear dispersion), tens of materials contradictorily show a measured temperature  $\kappa_L$  being even lower than  $\kappa_{L,\min}$  predicted by this model (Fig. 2; its  $n$ -dependence is discussed in the supplementary section entitled ‘Detailed deduction on phonon transport properties’). It should be noted that  $v_s$  and  $\bar{V}$  are respectively the sound velocity and average atomic volume, and the product  $v_s * \bar{V}^{-2/3}$  is the key parameter determining  $\kappa_{L,\min}$  (see the supplementary section entitled ‘Collective equations and mathematic code for  $\kappa_L$ -prediction in this work’) [48]. With the phonon

dispersion developed here, this work nicely eliminates the above contradiction.

## CONCLUSION

Taking into account the periodic boundary condition, a phonon dispersion and thus a time- and cost-effective phonon transport model are developed in this work, which significantly improves the accuracy for quickly predicting the lattice thermal conductivity ( $\kappa_L$ ) of solids. This offers an effective design for thermal functional solids. It further provides the theoretical possibility of  $\kappa_L$  being lower in many materials than is currently thought, validating further potential for advancing the thermal functionalities and thermal energy applications of solid materials.

## METHODS

Here we show brief deductions on phonon dispersion and transport properties taking into account the periodic boundary condition [47] (more details are given in the supplementary sections entitled ‘Detailed deduction on phonon transport properties’ and ‘Comparison on  $\kappa_L$  predicted by a Debye-Snyder model and the one developed in this work’). Considering the nearest-neighboring interactions, the phonon dispersion of a 1D single-atom chain is strictly a sine function (Equation S1a). Once the number of atoms in a primitive cell ( $n$ ) and the dimensionality of the material ( $d$ ) increase, the product of acoustic and optical dispersions yields a sine function (Equation S1b). This leads the dispersion of the acoustic branch to quickly approach a sine function when the mass and/or force contrast is large.

It is therefore reasonable to approximate the acoustic dispersion (frequency of  $\omega_{a,j}$  versus wave vector  $k$ ) for a material with a sound velocity of  $v_{s,j}$  (Equation S4) as

$$\omega_{a,j}(k) = \frac{2}{\pi} v_{s,j} k_c \sin\left(\frac{\pi k}{2 k_c}\right), \quad (1)$$

where  $j$  defines the polarizations of lattice vibrations (longitudinal or transverse) and  $k_c$  is the cut-off wave vector. In the case of  $n = 1$ , there is no optical branch, and the acoustic branch strictly has a dispersion of sine [47] (Fig. 1c). This means that the phonon group velocity ( $v_g$ , the slope of phonon frequency versus wave vector) is strongly frequency-dependent, which is further related to the sound velocity ( $v_s$ ) via Equation 1 (see the supplementary section entitled ‘Detailed deduction on phonon transport properties’). For simplicity the force constant and atomic mass are both averaged in

this work (see the supplementary section entitled ‘Detailed deduction on phonon transport properties’). This leads the phonon dispersion (frequency of  $\omega_{o,i,j}$  versus wave vector  $k$ ) of each optical branch to have a series of constant frequencies when  $n > 1$  (Fig. 1c). Both  $\omega_{o,i,j}$  and the effective group velocity ( $v_{\text{eff},i}$ ) are believed to be the ones at the median of wave vectors in the  $i$ th extended Brillouin zone for  $n = 1$ , since the case of  $n = \infty$  is the quantization of  $n = 1$  (Fig. 1c and the supplementary section entitled ‘Detailed deduction on phonon transport properties’). Note that a better understanding of phonon transport can be expected if the detailed dispersions on optical phonons are known (such as by first-principles calculations or inelastic neutron scattering measurements). The resulting equations for specific heat are given in the supplementary material (see the supplementary section entitled ‘Detailed deduction on phonon transport properties’).

At room temperature or above, the scattering of phonons is known to be dominated by inherent Umklapp processes due to the lattice anharmonicity in most solids. Considering this type of scattering only, the resulting relaxation time ( $\tau_U$ ; see the supplementary section entitled ‘Detailed deduction on phonon transport properties’) enables a determination of lattice thermal conductivity due to acoustic phonons via

$$k_{L,a} = \frac{1}{d} c_{V,a} v_g^2 \tau_U. \quad (2)$$

A constant frequency (i.e. flat dispersion) for each optical branch validates the approximation as the Einstein mode [57], leading the relaxation time to be half of the period ( $\tau_{\text{min}}$ ) of each phonon (see the supplementary section entitled ‘Detailed deduction on phonon transport properties’). This results in an optical lattice thermal conductivity ( $\kappa_{L,o}$ ) of

$$k_{L,o} = \sum_{i=2}^n \frac{1}{d} c_{V,o,i} v_{\text{eff},i}^2 \tau_{\text{min},o,i} \quad (3)$$

and a total lattice thermal conductivity ( $\kappa_L$ ) of  $\kappa_L = \kappa_{L,a} + \kappa_{L,o}$

When the scattering of acoustic phonons is maximized, the relaxation time is minimized to be half of the period of each phonon as well. This enables a prediction of minimal lattice thermal conductivity ( $\kappa_{L,\text{min}}$ ).

## SUPPLEMENTARY DATA

Supplementary data are available at [NSR](https://doi.org/10.1093/nsr/nwz014) online.

## ACKNOWLEDGEMENTS

The authors thank Prof. Gerald Jeffrey Snyder from Northwestern University and Prof. Donald T. Morelli from Michigan State University for their discussions.

## FUNDING

This work is supported by the National Key Research and Development Program of China (2018YFB0703600), the National Natural Science Foundation of China (11474219 and 51772215), the Fundamental Research Funds for Science and Technology Innovation Plan of Shanghai (18JC1414600), the Fok Ying Tung Education Foundation (20170072210001) and the ‘Shu Guang’ project supported by Shanghai Municipal Education Commission and Shanghai Education Development Foundation.

## REFERENCES

- Pernot G, Stoffel M and Savic I *et al.* Precise control of thermal conductivity at the nanoscale through individual phonon-scattering barriers. *Nat Mater* 2010; **9**: 491–5.
- Pature NP, Gell M and Jordan EH. Thermal barrier coatings for gas-turbine engine applications. *Science* 2002; **296**: 280–4.
- Bell LE. Cooling, heating, generating power, and recovering waste heat with thermoelectric systems. *Science* 2008; **321**: 1457–61.
- He J and Tritt TM. Advances in thermoelectric materials research: looking back and moving forward. *Science* 2017; **357**: eaak9997.
- Zhu T, Liu Y and Fu C *et al.* Compromise and synergy in high-efficiency thermoelectric materials. *Adv Mater* 2017; **29**: 1605884.
- Chiritescu C, Cahill DG and Nguyen N *et al.* Ultralow thermal conductivity in disordered, layered WSe<sub>2</sub> crystals. *Science* 2007; **315**: 351–3.
- Behabtu N, Young CC and Tsentelovich DE *et al.* Strong, light, multifunctional fibers of carbon nanotubes with ultrahigh conductivity. *Science* 2013; **339**: 182–6.
- Chen Z, Zhang X and Pei Y. Manipulation of phonon transport in thermoelectrics. *Adv Mater* 2018; **30**: 1705617.
- Lin S, Li W and Li S *et al.* High thermoelectric performance of Ag<sub>9</sub>GaSe<sub>6</sub> enabled by low cutoff frequency of acoustic phonons. *Joule* 2017; **1**: 816–30.
- Li W, Lin S and Weiss M *et al.* Crystal structure induced ultralow lattice thermal conductivity in thermoelectric Ag<sub>9</sub>AlSe<sub>6</sub>. *Adv Energy Mater* 2018; **8**: 1800030.
- Zhang X, Chen Z and Lin S *et al.* Promising thermoelectric Ag<sub>5–8</sub>Te<sub>3</sub> with intrinsic low lattice thermal conductivity. *ACS Energy Lett* 2017; **2**: 2470–7.
- Jiang B, Qiu P and Eikeland E *et al.* Cu<sub>9</sub>GeSe<sub>6</sub>-based thermoelectric materials with an argyrodite structure. *J Mater Chem C* 2017; **5**: 943–52.
- Vining CB. Silicon germanium. In: Rowe DM (ed.). *CRC Handbook of Thermoelectrics*. Boca Raton, FL: CRC Press, 1995, 329–37.
- Schemer H and Scherrer S. Bismuth telluride. antimony telluride. and their solid. In: Rowe DM (ed.). *CRC Handbook of Thermoelectrics*. Boca Raton, FL: CRC Press, 1995.
- Li J, Zhang X and Chen Z *et al.* Low-symmetry rhombohedral GeTe thermoelectrics. *Joule* 2018; **2**: 976–87.
- Li W, Lin S and Zhang X *et al.* Thermoelectric properties of Cu<sub>2</sub>SnSe<sub>4</sub> with intrinsic vacancy. *Chem Mater* 2016; **28**: 6227–32.
- Li W, Zheng L and Ge B *et al.* Promoting SnTe as an eco-friendly solution for p-PbTe thermoelectric via band convergence and interstitial defects. *Adv Mater* 2017; **29**: 1605887.
- Chen Z, Ge B and Li W *et al.* Vacancy-induced dislocations within grains for high-performance PbSe thermoelectrics. *Nat Commun* 2017; **8**: 13828.
- Chen Z, Jian Z and Li W *et al.* Lattice dislocations enhancing thermoelectric PbTe in addition to band convergence. *Adv Mater* 2017; **29**: 1606768.
- Kim SI, Lee KH and Mun HA *et al.* Dense dislocation arrays embedded in grain boundaries for high-performance bulk thermoelectrics. *Science* 2015; **348**: 109–14.
- Shuai J, Geng H and Lan Y *et al.* Higher thermoelectric performance of Zintl phases (Eu<sub>0.5</sub>Yb<sub>0.5</sub>)<sub>1-x</sub>Ca<sub>x</sub>Mg<sub>2</sub>Bi<sub>2</sub> by band engineering and strain fluctuation. *Proc Natl Acad Sci USA* 2016; **113**: E4125–32.
- Hsu KF, Loo S and Guo F *et al.* Cubic AgPb<sub>m</sub>SbTe<sub>2+m</sub>: bulk thermoelectric materials with high figure of merit. *Science* 2004; **303**: 818–21.
- Biswas K, He J and Blum ID *et al.* High-performance bulk thermoelectrics with all-scale hierarchical architectures. *Nature* 2012; **489**: 414–8.
- Morelli DT, Jovovic V and Heremans JP. Intrinsically minimal thermal conductivity in cubic I-V-VI<sub>2</sub> semiconductors. *Phys Rev Lett* 2008; **101**: 035901.
- Heremans JP. The anharmonicity blacksmith. *Nat Phys* 2015; **11**: 990–1.
- Li CW, Hong J and May AF *et al.* Orbitally driven giant phonon anharmonicity in SnSe. *Nat Phys* 2015; **11**: 1063–9.
- Li CW, Ma J and Cao HB *et al.* Anharmonicity and atomic distribution of SnTe and PbTe thermoelectrics. *Phys Rev B* 2014; **90**: 214303.
- Li W, Lin S and Ge B *et al.* Low sound velocity contributing to the high thermoelectric performance of Ag<sub>9</sub>SnSe<sub>6</sub>. *Adv Sci* 2016; **3**: 1600196.
- Ying P, Li X and Wang Y *et al.* Hierarchical chemical bonds contributing to the intrinsically low thermal conductivity in  $\alpha$ -MgAgSb thermoelectric materials. *Adv Funct Mater* 2017; **27**: 1604145.
- Slack GA. Thermal conductivity of pure and impure silicon, silicon carbide, and diamond. *J Appl Phys* 1964; **35**: 3460–6.
- Xu X, Pereira LF and Wang Y *et al.* Length-dependent thermal conductivity in suspended single-layer graphene. *Nat Commun* 2014; **5**: 3689.
- Wang M and Lin S. Ballistic thermal transport in carbyne and cumulene with micron-scale spectral acoustic phonon mean free path. *Sci Rep* 2016; **5**: 18122.

33. Eucken A. Über die Temperaturabhängigkeit der Wärmeleitfähigkeit fester Nichtmetalle. *Ann Phys* 1911; **339**: 185–221.
34. Debye PJW, Nernst W and Smoluchowski M *et al.* *Vorträge über die kinetische Theorie der Materie und der Elektrizität*. Leipzig: BG Teubner, 1914.
35. Peierls R. Zur kinetischen Theorie der Wärmeleitung in Kristallen. *Ann Phys* 1929; **395**: 1055–101.
36. Leibfried G and Schlömann E. Heat conduction in electrically insulating crystals. *Nachr Akad Wiss Gottingen Math Phys Klasse 2a* 1954; **71**: 71–93.
37. Julian CL. Theory of heat conduction in Rare-Gas crystals. *Phys Rev* 1965; **137**: A128–37.
38. Slack GA. The thermal conductivity of nonmetallic crystals. *Solid State Phys* 1979; **34**: 1–71.
39. Klemens PG. Thermal conductivity and lattice vibrational modes. *Solid State Phys* 1958; **7**: 1–98.
40. Callaway J. Model for lattice thermal conductivity at low temperatures. *Phys Rev* 1959; **113**: 1046–51.
41. Holland MG. Analysis of lattice thermal conductivity. *Phys Rev* 1963; **132**: 2461–71.
42. Tiwari MD and Agrawal BK. Analysis of the lattice thermal conductivity of germanium. *Phys Rev B* 1971; **4**: 3527–32.
43. Chung JD, McGaughey AJH and Kaviani M. Role of phonon dispersion in lattice thermal conductivity modeling. *J Heat Transfer* 2004; **126**: 376.
44. Dames C. Theoretical phonon thermal conductivity of Si/Ge superlattice nanowires. *J Appl Phys* 2004; **95**: 682–93.
45. Toberer E, Zevalkink A and Snyder GJ. Phonon engineering through crystal chemistry. *J Mater Chem* 2011; **21**: 15843–52.
46. Debye P. Zur Theorie der spezifischen Wärmen. *Ann Phys* 1912; **344**: 789–839.
47. Born M and Von Karman T. Vibrations in space gratings (molecular frequencies). *Z Phys* 1912; **13**: 297–309.
48. Cahill DG and Pohl R. Heat flow and lattice vibrations in glasses. *Solid State Commun* 1989; **70**: 927–30.
49. Ong WL, O'Brien ES and Dougherty PS *et al.* Orientational order controls crystalline and amorphous thermal transport in superatomic crystals. *Nat Mater* 2017; **16**: 83–8.
50. Simon SH. *The Oxford Solid State Basics*, 1st edn. Oxford: Oxford University Press, 2013.
51. Liu H, Shi X and Xu F *et al.* Copper ion liquid-like thermoelectrics. *Nat Mater* 2012; **11**: 422–5.
52. Li B, Wang H and Kawakita Y *et al.* Liquid-like thermal conduction in intercalated layered crystalline solids. *Nat Mater* 2018; **17**: 226–30.
53. Slack GA. Nonmetallic crystals with high thermal conductivity. *J Phys Chem Solids* 1973; **34**: 321–35.
54. Roufosse M and Klemens PG. Thermal conductivity of complex dielectric crystals. *Phys Rev B* 1973; **7**: 5379–86.
55. Tritt TM. *Thermal Conductivity: Theory, Properties, and Applications*. Springer Science & Business Media, 2005.
56. Agne MT, Hanus R and Snyder GJ. Minimum thermal conductivity in the context of diffusion-mediated thermal transport. *Energy Environ Sci* 2018; **11**: 609–16.
57. Einstein A. Elementare Betrachtungen über die thermische Molekularbewegung in festen Körpern. *Ann Phys* 1911; **340**: 679–94.